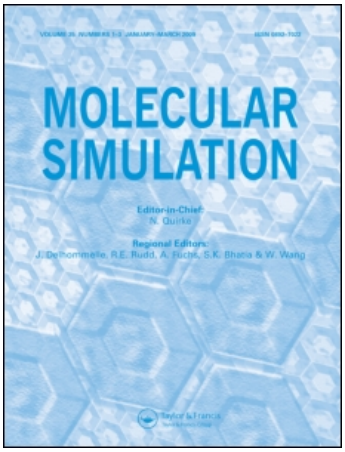

Molecular Simulation
Publication details, including instructions for authors and subscription information:
http://www.informaworld.com/smpp/title~content=t713644482

Simulation of the hydration structure of glycyl-alanine

T. Liang[a]; T. R. Walsh[a]
[a] Department of Chemistry and Centre for Scientific Computing, University of Warwick, Coventry, UK

To cite this Article Liang, T. and Walsh, T. R.(2007) 'Simulation of the hydration structure of glycyl-alanine', Molecular Simulation, 33: 4, 337 — 342
To link to this Article: DOI: 10.1080/08927020601155378
URL: http://dx.doi.org/10.1080/08927020601155378

Molecular Simulation, Vol. 33, Nos. 4–5, 15–30 April 2007, 337–342

Taylor & Francis
Taylor & Francis Group

Simulation of the hydration structure of glycyl-alanine

T. LIANG* and T. R. WALSH

Department of Chemistry and Centre for Scientific Computing, University of Warwick, Coventry CV4 7AL, UK

(Received June 2006; in final form October 2006)

Molecular dynamics (MD) simulations studies have been performed on the aqueous solvation of the dipeptide glycyl-alanine (GA) using classical force-fields AMBER (J. Wang, P. Cieplak, P. A. Kollman, *J. Comp. Chem.* 21, 1049 (2000)) and CHARMM (N. Foloppe, A. D. MacKerell, *J. Comp. Chem.* 21, 86 (2000)), and the polarizable force-field AMOEBAPRO (P. Ren, J. W. Ponder, *J. Comp. Chem.* 23, 1497 (2002), P. Ren, J. W. Ponder, *J. Phys. Chem. B.* 107, 5933 (2003)). Radial distribution functions and hydration numbers are calculated and compared with the data from Car-Parrinello molecular dynamics (CPMD) and experiments. Our results show all three force-fields can reproduce most of the features of the hydration structure of dipeptide GA. It is also found that AMBER and CHARMM force-fields can describe an averaged chemical environment, while AMOEBAPRO force-field has the capability of capturing the changes in the local environment caused by conformational transitions.

Keywords: Molecular dynamics; Polarizable force-field; Hydration structure

1. Introduction

The interaction between protein and water plays an important role in protein activity [1–3]. There has been a recent growth in the number of studies investigating the interaction and hydration structure around proteins and peptides under aqueous conditions using experiment and theoretical methods [4–9]. In particular, molecular dynamics (MD) simulations provide a very useful tool to study the dynamic process of the hydration structure at atomistic level.

It is crucial in MD simulations to use accurate force-fields in order to reproduce experimental results. Traditional force-fields for bulk systems are usually parameterized against bulk properties with implicit inclusion of multibody effects such as polarization. Although this kind of force-field has been proven successful in many cases, a single set of fixed charges is not generally accurate when applied to some dramatic change in chemical environment, such as inter- or intra-molecular polarization caused by conformation transitions or molecular adsorption [10–12].

It has been found that widely-used force-fields typically yield hydration structures of peptide groups that are not entirely consistent with available experiment data or density-functional theory simulation (CPMD) [13–16]. Previous simulations [15,17,18] using AMBER or CHARMM yielded a hydration number for the carboxylate group of around 6.6–7.2 per carboxylate, which is one hydration bond more than the CPMD result and experiments suggest. Hugosson *et al.* [19] found the water distribution around the terminal NH_3^+ and COO^- groups of peptides could not be described properly by the traditional force-fields.

Polarizable potentials have shown promising results compared with traditional force-fields [20–24]. The polarizable AMOEBAPRO force-field [11,26], based on a distributed-multipole description of the electrostatics, has been developed to describe the variable chemical environment in proteins more accurately. The polarizable water model AMOEBA [25], used in this work, shows an excellent agreement with experimental and *ab initio* results for various conditions, such as clusters, liquid water and ice. The application of the AMOEBAPRO model has been shown to successfully capture much of the intra-molecular polarization caused by conformational transitions [26]. In our previous work [27] using the polarizable AMOEBAPRO force-field, it has been found that the solvation structure of the carboxylate within the dipeptide aspartyl-alanine acid is in very good agreement with CPMD results and experimental data.

*Corresponding author. Email: t.liang@warwick.ac.uk

Molecular Simulation
ISSN 0892-7022 print/ISSN 1029-0435 online © 2007 Taylor & Francis
http://www.tandf.co.uk/journals
DOI: 10.1080/08927020601155378

In this work, we focus on the hydration structure around individual groups within the dipeptide glycyl-alanine (GA). *Ab initio* calculations show the water adsorption process involves a significant conformational change in glycyl-alanine dipeptides [28]. Our previous work has indicated the hydration number of the carboxylate group in aspartyl-alanine changes depending on different conformations of the backbone [27]. In this work, we have used several different initial conformations of GA in MD simulations in order to investigate the conformational influence on the hydration structure in AMOEBAPRO, AMBER and CHARMM force-fields. The hydration structure around each group within the dipeptide is characterized by radial distribution functions (RDFs) and compared with the CPMD and experimental data. Our results show that most of the hydration structures around GA could be reproduced by these three force-fields. The AMBER and CHARMM force-fields produce averaged influences from the bulk system. The simulation results from AMOEABPRO force-field suggest the hydration structure is affected by the local environment caused by the conformational change.

2. Methods

The structure of GA is shown in figure 1. The backbone torsions are, by convention, defined as ϕ, ω and ψ. Three different initial conformations were adopted. The first one has ϕ, ω and ψ dihedral angles of 225, 180, and 135°, respectively. This structure is labeled as C1 herein. The simulation starting with the C1 structure is referred to as the C1 simulation. The second structure has ϕ, ω and ψ dihedral angles of 300, 230 and 300°, respectively and is labelled as C2. The third structure adopted is with dihedral angles of 300, 180 and 180° and labelled as C3. The C2 and C3 structures are found to be favoured for adsorption of water, as suggested by *ab initio* calculations [28].

Three different kinds of force-field were chosen for these simulations. The first one is the AMOEBAPRO force-field developed by Ponder and co-workers [11,25,26]. This force-field employs distributed multipoles for electrostatic contributions, and includes intra- and inter-molecular induction contributions. The intra-molecular induction term is novel and accounts for changes in multipole moments that arise due to molecular flexibility. The polarization effects are explicitly treated using isotropic dipole polarizabilities. Repulsion–dispersion interactions between pairs of non-bonded atoms are represented by a buffered 14–7 potential. Both the dipeptide and the water molecules are described using this force-field. Further details of the force-field can be obtained from the previous work of Ren and Ponder [11,25,26]. The other two force-fields used here are AMBER99 [29] and CHARMM27 [30,31] which are traditional force-fields that are widely used in protein simulation. The water model used in the AMBER and CHARMM simulations was TIP3P [32]. All calculations were performed using the TINKER [33] software package.

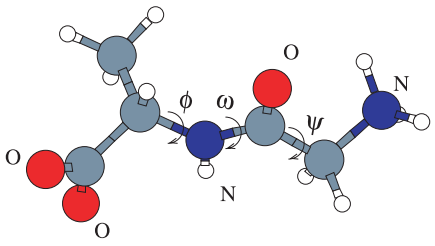

Figure 1. Molecular structure of glycyl-alanine (GA), with dihedral ϕ, ω and ψ marked as shown.

The GA and 164 water molecules were randomly put into a periodic cell with an initial density of about 0.75 g/ml and a system concentration of 0.34 M. Minimization was then applied to the cubic cell to eliminate strong forces among atoms. High pressure NPT simulation was followed to compress the density to a reasonable value near 1.0 g/ml. Newton's equations of motion were integrated using the Verlet algorithm [34] in the isothermal–isobaric (NPT) ensemble. Thermostatting was achieved using the Nosé–Hoover algorithm [35–37] with a coupling constant of 0.2 ps for the temperature bath and 1.0 ps for the pressure bath. Pressure of 1 atm and a temperature of 298 K were the conditions set throughout all simulations. The time step used in this simulation was 1 fs with coordinates saved every 0.5 ps. The typical system dimensions amounted to a box with side length of roughly 17.6 Å. This system was equilibrated with runs of 100 ps for AMOEBAPRO, 500 ps for AMBER and CHARMM, with production runs of 1 ns for all three cases.

3. Results and discussion

3.1 Conformational sampling

The dihedral angles ϕ, ω, ψ of GA were sampled in the MD simulations. Figure 2 shows the torsion distributions for the simulations starting from the three different initial

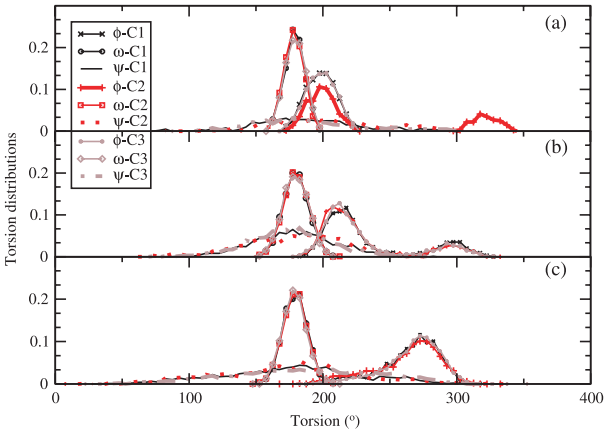

Figure 2. Backbone torsion distributions starting from three different initial conformations using three different force-fields. (a) AMOEBAPRO; (b) AMBER; (c) CHARMM.

conformations using different force-fields. For the AMOEBAPRO force-field, ϕ has very similar torsion distributions amongst the C1 and C3 simulations, with only one single peak found at around 200° for each simulation. However, two peaks appear in the torsion distribution of dihedral ϕ for the C2 simulation located at 200 and 320°. The middle ω shows a narrow distribution near 180° as to be expected. The ψ has a very broad torsion distribution in the range from 30 to 330°. Because only one part of the torsion distribution of the dihedral ϕ was found in the C1 and C3 simulations within the 1ns timescale of the simulations, GA in aqueous solution is considered unable to explore the same conformational space from different conformations using AMOEBAPRO force-field.

Figure 2(b),(c) shows torsion distributions for the AMBER and CHARMM force-fields. The ϕ, ω, ψ dihedrals have very similar distributions regardless of initial structures for both force-fields. Two peaks from the torsion distribution of dihedral ϕ in figure 2(b) were found at about 212 and 295°. The ϕ distribution for the CHARMM force-field in figure 2(c) only presents a single peak with a wide range between 200 and 300°. This peak is located in the *gauche* state range around 275°. Although most of the torsions are *gauche*, the asymmetrical shape of the distribution curve between 180 and 240° indicates some of the torsions are located in the *trans* state range.

Generally, the dihedrals ϕ, ω, ψ for the three force-fields could explore the same conformational space during the MD simulation. ϕ always is located in *trans* or *gauche* state. The dihedral ω stays narrowly at around 180° in all simulations as to be expected for a peptide bond. The dihedral ψ shows a very wide distribution between 50 and 300°.

The CPMD calculation [19] for GA shows ϕ has two peaks at around 210–200° and 290–300° and dihedral ψ distribution is in the range about 120–240°. It is also noticed that the CPMD simulation could not provide enough sampling time for the torsion distribution.

For the small dipeptide GA, the initial conformations were found to be not important to the AMBER and CHARMM force-fields, since the molecule could convert among different states to explore conformational space. However, the torsions are more restrained in AMOEBAPRO force-field. Only the C2 simulation explores the same conformational space as that in the other force-fields. One possible reason is that AMBER and CHARMM have implicit multibody effects which are averaged over the conformation space in the bulk system, which allow conformational transitions to take place more easily. The conformation dependence of electrostatics from the explicit polarization term in the AMOEBAPRO force-field leads to a complex situation for each torsion, which might cause some dihedrals to remain more easily locked in one state than that with averaged electrostatics. The simulation results suggest initial conformations should be considered carefully in MD simulations using polarizable force-fields.

3.2. Hydration structures

Since the C1 and C3 simulations using the AMOEBAPRO force-field produced only part of the torsion distributions, the trajectory from C2 was used for further analysis. The influence from different conformations will be discussed later. For the AMBER and CHARMM force-fields, only the trajectories from the C1 simulation were adopted for the analysis since the C1, C2 and C3 simulations explored the same conformation space.

The hydration structure around different regions of GA is allocated to several functional groups. These are the terminal COO^- group, the terminal NH_3^+ group, and the NH group and the CO group in the peptide bond. The hydration number for each group is calculated by integrating all water molecules inside the first solvation shell, where the cutoff distance 2.5 Å is adopted for all simulations. An estimated error is calculated by taking the average of the difference of hydration numbers from radius 2.30 to 2.70 Å. For the COO^- group, the hydration number for oxygen atoms is calculated individually. The same treatment is applied for the three hydrogen atoms in NH_3^+ group.

RDFs between oxygen atoms of the carboxylate and the water are shown in figure 3(a). The height of the first peak is much lower from the AMOEBAPRO simulations than that from CHARMM and AMBER. The peak position also is moved a little outwards in AMOEBAPRO. The RDFs from the AMBER and CHARMM force-fields are very similar to each other. Compared with the CPMD data [19], the AMOEBAPRO force-field shows the most similarity. The same trend has been found in our previous work for the dipeptide aspartyl-alanine [27].

Table 1 shows the hydration numbers of the four groups of GA using the different force-fields. The hydration number for each oxygen atom of the carboxylate is 2.68 for the AMOEBAPRO force-field, which is closer to 2.50 from the CPMD result. The AMBER and CHARMM results apparently overestimate hydration number by 34 and 48%, respectively. A similar discrepancy between

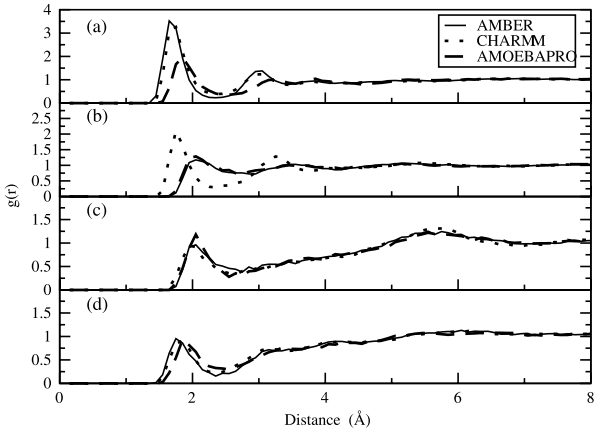

Figure 3. Radial distribution functions for the interaction between the individual group of GA and water molecules. (a) COO^- and H(w); (b) NH_3^+ and O(w); (c) NH and O(w); (d) CO and H(w).

Table 1. Hydration number, N_w, of selected groups of the dipeptide glycyl-alannine.The radius of the first solvation shell is 2.50 Å. The value in parentheses is the estimated absolute error by averaging the difference of hydration numbers if the radius is 2.30 or 2.70 Å.

	AMOEBAPRO	*AMBER*	*CHARMM*	*CPMD*
O_{COO^-}	2.68 (0.06)	3.34 (0.13)	3.70 (0.20)	2.5[†]/2.35[‡]
$H_{NH_3^+}$	1.33 (0.02)	1.25 (0.02)	1.17 (0.07)	1.0[†]
H_{NH}	0.91 (0.02)	0.88 (0.01)	0.88 (0.01)	1.0[†]
O_{CO}	1.48 (0.05)	1.34 (0.08)	1.41 (0.01)	1.3/1.6/1.1[¶]

[†] Ref. [19]. [‡] Ref. [14]. [¶] Different hydration number obtained from different initial conformations in Ref. [19].

traditional force-fields and CPMD has been noted by our previous work [27] and others [13,19]. The nuclear magnetic resonance (NMR) studies of frozen polypeptide solutions [38] yield a hydration number of 2.50–3.25 per oxygen atom of carboxylate group. Neutron scattering and X-ray experiments [39] suggest a hydration number of 2.2 in HCOONa solution. CPMD simulations [14] for aqueous glycine found 2.35 hydrogen bonds per oxygen atom of carboxylate group. Our simulations show all three force-fields overestimate the hydration number of carboxylate. Combining the RDFs result, hydration structures of the carboxylate group from the AMOEBAPRO force-field show the closest agreement with results from CPMD and experiments.

Figure 3(b) shows the RDFs between hydrogen atoms of the terminal NH_3^+ group and water oxygen atoms. The CHARMM force-field has a more compact first solvation shell which has the peak height of 2.10 and peak position at about 1.75 Å. The first peak from AMOEBAPRO is located at about 2.05 Å with a height of 1.29. The peak position from AMBER is at about 2.05 and the peak height is 1.17. A similiar MD simulation of GA using AMBER force-field (parm98) presented the first peak with the position of about 2.02 Å and the height 1.50 [19]. Compared among these three force-fields, the attraction between hydrogen atoms of NH_3^+ and oxygen atoms of water in CHARMM is relatively stronger. The CPMD simulation [19] of GA found the peak position is at about 2.0 Å and the peak height ranges between 0.8 and 2.0 from different simulation conditions. The first peak of $g_{H_{NH_3}-O_w}(r)$ of glycine in another CPMD simulations [14] is at around 2 Å with a height of 1.4. Simulations of $CH_3NH_3^+$ in water using MC simulations [18] have the peak position at around 1.9 Å. Therefore, the AMOEBAPRO and AMBER force-fields underestimate the $H_{(NH_3)}\cdots O(w)$ interaction and put the first solvation shell further away from the hydrogen atoms.

The average hydration number for the hydrogen atom of NH_3^+ in table 1 is 1.33, 1.25 and 1.17 for AMOEBAPRO, AMBER and CHARMM, respectively. NMR studies [38] suggest 1.17 water molecules per hydrogen for the ammonium group in lysine. It also was noted from CPMD simulations [14] that 1.00 water molecules were assigned to each hydrogen atom in NH_3^+ of glycine. The hydration number from another MD simulation [19] with the AMBER force-field (parm98) and TIP3P water is about 1.20. For the NH_3^+ group of $CH_3NH_3^+$, MD simulations based on the AMBER force-field and SPC/E water [15] revealed a hydration number of 1.22 per hydrogen atom. Monte Carlo (MC) simulations using TIP4P water yield hydration numbers of 1.17 [17] and 1.30 [18]. Therefore, in view of these results, the hydration numbers obtained in this work for all three force-fields are reasonably close to the results from experiments and other simulations.

The RDFs between the hydrogen atom of the NH group and water oxygen atoms are shown in figure 3(c). The position of the first peak from all force-fields is very similar, which is about 2.00 Å. The peak height from AMOEBAPRO is a greater than the others, at about 1.18. CPMD data give the distance between H and O from 1.6 to 2.5 Å with at peak at approximately 1.9 and a very diffuse second shell structure. The hydration number of the backbone NH group is found to be about 0.91, 0.88 and 0.88 for AMOEBAPRO, AMBER and CHARMM force-fields, respectively, as listed in Table 1. The CPMD results [19] report a hydration number of 1.0 with a fluctuation 0.2 about for the NH group in aqueous GA. Therefore, $g_H - O_w(r)$ and the hydration number from CPMD simulations is well reproduced by all three force-fields.

Figure 3(d) presents the RDFs between oxygen atoms of the backbone CO group and water hydrogen atoms. The position of the first peak from AMOEBAPRO is pushed outward farther compared with the other two force-fields. CPMD data show the position of the first peak is around 1.9 Å with a peak height of 1.0. Therefore, the first solvation shell structure from the three force-fields is considered to agree with the CPMD simulations.

Table 1 lists the hydration numbers of the backbone CO group, which are 1.48 from AMOEBAPRO, 1.34 from AMBER and 1.41 from CHARMM. Since the hydration numbers from CPMD have a wide range from 1.1 to 1.6 depending on different simulation conditions, our results from the three force-fields are considered to all agree with the CPMD result.

3.3. Conformational effect on hydration structure of dipeptide CO group

It has been noted that a large fluctuation of 40–50% in the hydration number for the NH and CO groups occurs if different initial conformations are adopted in the CPMD simulations [19]. In our previous work, a conformational influence has been noted for the AMOEBAPRO force-field. In this work we have focused on the conformational influence on the hydration structure of the CO group.

The torsion distribution of the dihedral ϕ has been found to be located in *trans* and *gauche* states in all three force-fields. Therefore, new simulations using umbrella sampling were performed in which ϕ was restrained only to be in the *trans* state or the *gauche* state. The simulation is denoted as a *trans*-ϕ-simulation if ϕ is within the *trans* state and a *gauche*-ϕ-simulation if ϕ keeps in the *gauche* state. AMOEBAPRO and AMBER force-fields were used for these simulations.

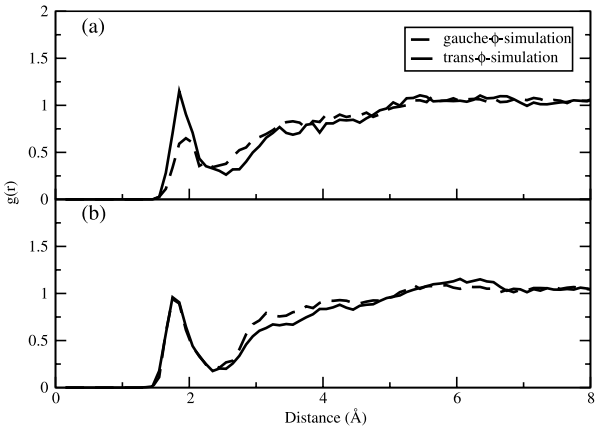

Figure 4. Radial distribution functions for the interaction between the backbone CO group and water molecules for the torsion-constraint simulations using different force-fields. (a) AMOEBAPRO; (b) AMBER.

Figure 4 shows the RDFs between the oxygen atom of the CO group and the water hydrogen atoms with the torsion restraint. The solid line in figure 4(a) represents the RDF when ϕ is restrained in the *trans* state using the AMOEBAPRO force-field and the dotted line represents ϕ is in the *gauche* state. The first peak height in the *trans*-ϕ-simulation is about 1.15, which is much higher than the peak height of 0.65 in the *gauche*-ϕ-simulation. Figure 4(b) shows there is only a slight difference in the first peak for both simulations when the AMBER force-field is applied.

Figure 5 presents two snapshots from the *trans*-ϕ-simulation and the *gauche*-ϕ-simulation using the AMOEBAPRO force-field. When the dihedral ϕ is *trans*, the average distance between oxygen atoms of the carboxylate and the oxygen atom of CO is about 5.04 Å. This distance would decrease to 3.35 Å when ϕ adopts the *gauche* state. The hydration number around the CO group drops from 1.61 ($\pm$0.02) to 1.26 ($\pm$0.13) with this conformation change. For the AMBER force-field, this distance decreases from 4.89 to 3.73 Å when ϕ changes from the *gauche* state to the *trans* state. However, the hydration number is found to only change slightly from 1.36 ($\pm$0.11) to 1.35 ($\pm$0.07). The torsion distributions of the dihedral ω and ψ are similar to the previous result without torsion restraint. So the difference of RDF and hydration number in the AMOEBAPRO force-field is proposed to be caused by the torsion change of the dihedral ϕ. When the CO group and the carboxylate approach each other, the electrostatic and steric effects could disturb the local distribution of water molecules.

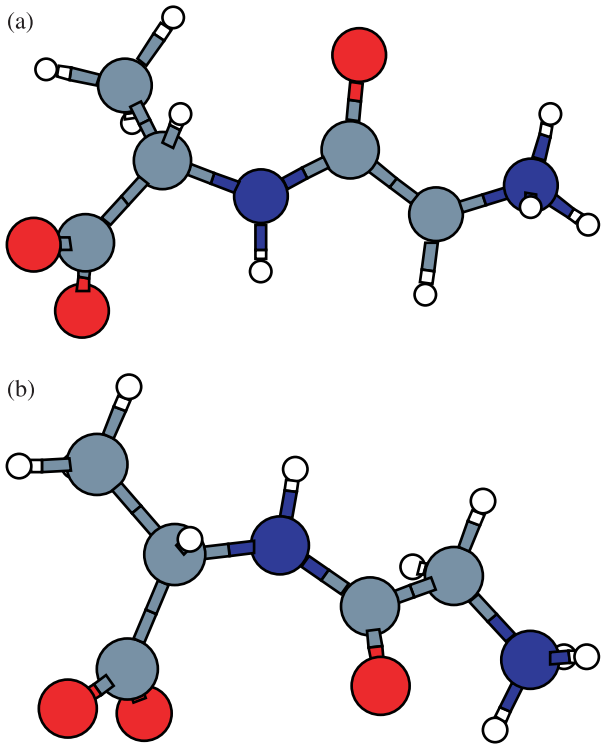

Figure 5. Typical conformations from the torsion-constraint simulation using the AMOEBAPRO force-field: (a) *trans*-ϕ-simulation; (b) *gauche*-ϕ-simulation.

Despite the big difference in hydration number caused by the conformation in the AMOEBAPRO force-field, the average value is about 1.44, which is close to the averaged hydration number of 1.36 from the AMBER force-field. Therefore, using the AMOEBAPRO force-field can distinguish the difference in the hydration structure of the CO group caused by the conformational changes.

4. Conclusions

In summary, we have used MD simulations to examine the hydration structure around functional groups of GA. Three kinds of force-fields were employed: AMOEBAPRO (with atomic polarizablities), AMBER and CHARMM force-fields. RDF results show that the patterns of the first solvation shell are similarly reproduced by all three force-fields compared with the CPMD data. The position and height of the first peak in the hydration structure of the backbone groups could be well described in these three force-fields. No single force-field performs well for both of the terminal groups. It was found that AMOEBAPRO could recover very well the water distribution around terminal carboxylate group and CHARMM does very well for the NH_3^+ group in comparison with the CPMD result.

The backbone dihedral angle distributions and hydration structures show that the AMBER and CHARMM force-fields could generate a more averaged environment for GA because of the rotation of the backbone torsions. The AMOEBAPRO force-field is more able to capture the specific chemical features and provide more details of the hydration structure. However, conformations in the MD simulations using AMOEBAPRO were found to more easily remain in one torsional state by the local environment and different initial conformations must be used to explore conformational space more thoroughly.

Acknowledgements

The authors gratefully acknowledge the computing facilities of the Centre for Scientific Computing, University of Warwick. This project is funded by the EPSRC Materials Modelling Consortium "Modelling the Biological Interface with Materials", GR/S80127/01.

References

[1] Y.K. Cheng, P.J. Rossky. Surface topography dependence of biomolecular hydrophobic hydration. *Nature*, **392**, 696 (1998).
[2] S. Balasubramaniam, S. Pal, B. Bagchi. Hydrogen-bond dynamics near a micellar surface: Origin of the universal slow relaxation at complex aqueous interfaces. *Phys. Rev. Lett.*, **89**, 115505 (2002).
[3] R.M. Daniel, R.V. Dunn, J.L. Finney, J. Smith, J.C. Annu. The role of dynamics in enzyme activity. *Rev. Biophhys. Biomol. Struct.*, **32**, 69 (2003).
[4] J.S. Klassen, P. Kebarle. Collision-induced dissociation threshold energies of protonated glycine, glycinamide, and some related small peptides and peptide amino amides. *J. Am. Chem. Soc.*, **119**, 6552 (1997).
[5] E.F. Strittmatter, E.R. Williams. Computational approach to the proton affinities of gly(n) (n = 1–10). *Int. J. Mass. Spectrom.*, **187**, 935 (1999).
[6] C. Schröder, T. Rudas, S. Boresch, O. Steinhauser. Simulation studies of the protein-water interface. i. Properties at the molecular resolution. *J. Chem. Phys.*, **124**, 234907 (2006).
[7] D. Russo, R.K. Murarka, J.R.D. Copley, T. Head-Gordon. Molecular view of water dynamics near model peptides. *J. Phys. Chem. B.*, **109**, 12966 (2005).
[8] M.B. Enright, X. Yu, D.M. Leitner. Hydration dependence of the mass fractal dimension and anomalous diffusion of vibrational energy in proteins. *Phys. Rev. E*, **73**, 051905 (2006).
[9] J. Knab, J. Chen, A. Markelz. Hydration dependence of conformational dielectric relaxation of lysozyme. *Biophys. J.*, **90**, 2576 (2006).
[10] O. Engkvist, P. Åstrand, G. Karlström. Accurate intermolecular potentials obtained from molecular wave functions: Bridging the gap between quantum chemistry and molecular simulations. *Chem. Rev.*, **100**, 4087 (2000).
[11] J.W. Ponder, D.A. Case. Force fields for protein simulation. *Adv. Protein Chem.*, **66**, 27 (2003).
[12] G.G. Ferenczy, P.J. Winn, C.A. Reynolds. Towards improved force fields. ii. Effective distributed multipoles. *J. Phys. Chem. A.*, **101**, 5446 (1997).
[13] K. Leung, S.B. Rempe. *Ab initio* molecular dynamics study of formate ion hydration. *J. Am. Chem. Soc.*, **126**, 344 (2004).
[14] K. Leung, S.B. Rempe. *Ab initio* molecular dynamics study of glycine intramolecular proton transfer in water. *J. Chem. Phys.*, **122**, 184506 (2005).
[15] E.C. Meng, P.A. Kollman. Molecular dynamics studies of the properties of water around simple organic solutes. *J. Phys. Chem.*, **100**, 11460 (1996).
[16] F.M.L.G. Stamato, J.M. Goodfellow. Computer simulation of amino-acid Zwitterions in solution. *Int. J. Quant. Chem.*, 277 (1986).
[17] G. Alagona, C. Ghio, P. Kollman. Monte carlo simulation studies of the solvation of ions. 1. Acetate anion and methylammonium cation. *J. Am. Chem. Soc.*, **108**, 185 (1986).
[18] W.L. Jorgensen, J.L. Gao. Monte Carlo simulations of the hydration of ammonium and carboxylate ions. *J. Phys. Chem.*, **90**, 2174 (1986).
[19] H.W. Hugosson, A. Laio, P. Maurer, U. Rothlisberger. A comparative theoretical study of dipeptide solvation in water. *J. Comp. Chem.*, **27**, 672 (2006).
[20] J.W. Caldwell, P.A. Kollman. Structure and properties of neat liquids using nonadditive molecular dynamics: Water, methanol, and N-methylacetamide. *J. Phys. Chem.*, **99**, 6208 (1995).
[21] H. Guo, N. Gresh, B.P. Roques, D.R. Salahub. Many-body effects in systems of peptide hydrogen-bonded networks and their contributions to ligand binding: A comparison of the performances of DFT and polarizable molecular mechanics. *J. Phys. Chem. B.*, **104**, 9746 (2000).
[22] C.J. Burnham, S.S. Xantheas. Development of transferable interaction models for water. iii. Reparametrization of an all-atom polarizable rigid model (TTM2-R) from first principles. *J. Chem. Phys.*, **116**, 1500 (2002).
[23] O. Engkvist, P.-O. Åstrand, G. Karlstörm. Intermolecular potential for the 1,2-dimethoxyethane-water complex. *J. Phys. Chem.*, **100**, 6950 (1996).
[24] G.G. Ferenczy, C.A. Reynolds. Modeling polarization through induced atomic charges. *J. Phys. Chem. A.*, **105**, 11470 (2001).
[25] P. Ren, J.W. Ponder. A consistent treatment of inter- and intramolecular polarization in molecular mechanics calculations. *J. Comp. Chem.*, **23**, 1497 (2002).
[26] P. Ren, J.W. Ponder. Polarizable atomic multipole water model for molecular mechanics simulation. *J. Phys. Chem. B.*, **107**, 5933 (2003).
[27] T. Liang, T. Walsh. Molecular dynamics simulations of peptide carboxylate hydration. *Phys. Chem. Chem. Phys.*, **8**, 4410 (2006).
[28] M. Kohtani, G.A. Breaux, M.F. Jarrold. Water molecule adsorption on protonated dipeptides. *J. Am. Chem. Soc.*, **126**, 1206 (2004).
[29] J. Wang, P. Cieplak, P.A. Kollman. How well does a restrained electrostatic potential (resp) model perform in calculating conformational energies of organic and biological molecules?. *J. Comp. Chem.*, **21**, 1049 (2000).
[30] A.D. MacKerell, D. Bashford, M. Bellott, R.L. Dunbrack, J.D. Evanseck, M.J. Field, S. Fischer, J. Gao, H. Guo, S. Ha, D. Joseph-McCarthy, L. Kuchnir, K. Kuczera, F.T.K. Lau, C. Mattos, S. Michnick, T. Ngo, D.T. Nguyen, B. Prodhom, W.E. Reiher, B. Roux, M. Schlenkrich, J.C. Smith, R. Stote, J. Straub, M. Watanabe, J. Wiorkiewicz-Kuczera, D. Yin, M. Karplus. All-atom empirical potential for molecular modeling and dynamics studies of proteins. *J. Phys. Chem. B.*, **102**, 3586 (1998).
[31] N. Foloppe, A.D. MacKerell. Jr. all-atom empirical force field for nucleic acids: i. parameter optimization based on small molecule and condensed phase macromolecular target data. *J. Comp. Chem.*, **21**, 86 (2000).
[32] W.L. Jorgensen, J. Chandraesekhar, J.W. Madura, R.W. Impey, M.L. Klein. Comparison of simple potential functions for simulating liquid water. *J. Chem. Phys.*, **79**, 926 (1983).
[33] J.W. Ponder, P. Ren, R.V. Pappu, R.K. Hart, M.E. Hodgson, D.P. Cistola, C.E. Kundrot, F.M. Richards. *TINKER—Software Tools for Molecular Design*, St. Louis, MO, version 4.2 ed. (2004).
[34] L. Verlet. Computer "experiments" on classical fluids. i. thermodynamical properties of lennard–jones molecules. A unified formulation of the constant temperature molecular dynamics methods. *Phys. Rev.*, **159**, 98 (1967).
[35] S. Nosé. A unified formulation of the constant temperature molecular dynamics methods. *J. Chem. Phys.*, **81**, 511 (1984).
[36] S. Nosé. A molecular dynamics method for simulations in the canonical ensemble. *Mol. Phys.*, **52**, 255 (1984).
[37] G.H. Hoover. Canonical dynamics: Equilibrium phase-space distributions. *Phys. Rev. A*, **31**, 1695 (1985).
[38] I.D. Kuntz. Hydration of macromolecules. iii. Hydration of polypeptides. *J. Am. Chem. Soc.*, **93**, 514 (1971).
[39] Y. Kameda, T. Mori, T. Nishiyama, T. Usuki, O. Uemura. Structure of concentrated aqueous sodium formate solution. *Bull Chem. Soc. Jpn.*, **69**, 1495 (1996).